CrossMark

ORIGINAL ARTICLE

Searching for some natural orbits to observe the double asteroid 2002CE$_{26}$

Bruna Yukiko Pinheiro Masago Mescolotti[1] (ORCID) ·
Antonio Fernando Bertachini de Almeida Prado[1] · Ana Paula Marins Chiaradia[2] ·
Vivian Martins Gomes[2]

Abstract Knowledge of the Solar System is increasing with data coming from space missions to small bodies. A mission to those bodies offers some problems, because they have several characteristics that are not well known, like their shapes, sizes and masses. The present research has the goal of searching for trajectories around the double asteroid 2002CE$_{26}$, a system of Near-Earth Asteroids (NEAs) of the Apollo type. For every trajectory of the spacecraft, the evolution of the distances between the spacecraft and the two bodies that compose the system is crucial, due to its impact in the quality of the observations made from the spacecraft. Furthermore, this study has a first objective of searching for trajectories that make the spacecraft remain as long as possible near the two bodies that compose the asteroid system, without the use of orbital maneuvers. The model used here assumes elliptical orbits for the asteroids. The effect of the solar radiation pressure is also included, since it is a major perturbing force acting in spacecrafts traveling around small bodies. The natural orbits found here are useful for the mission. They can be used individually or combined in several pieces by orbital maneuvers. Another point considered here is the importance of the errors in the estimation of the physical parameters of the bodies. This task is very important, because there are great uncertainties in these values because the measurements are based on observations made from the Earth. It is shown that a variation of those parameters can make very large modifications in the times that the spacecraft remains close to the bodies of the system (called

✉ B.Y.P.M. Mescolotti
  brunamasago@gmail.com

[1] National Institute for Space Research (INPE), São José dos Campos, SP, Brazil

[2] School of Engeneering, São Paulo State University (UNESP), Guaratinguetá, SP, Brazil

here "observational times"). Those modifications are large enough to make the best trajectories obtained under nominal conditions to be useless under some errors in the physical parameters. So, a search is made to find trajectories that have reasonable observation times for all the assumed error scenarios for the two bodies, because those orbits can be used as initial parking orbits for the spacecraft. We called these orbits "quasi-stable orbits", in the sense that they do not collide with any of the primaries nor travel to large distances from them. From these orbits, it is possible to make better observations of the bodies in any scenario, and a more accurate estimation of their sizes and masses is performed, so giving information to allow for other choices for the orbit of the spacecraft.

1 Introduction

Asteroids are small bodies located in the Solar System. Most of them are located in a region called "main belt of asteroids". This region is located between the orbits of Mars and Jupiter. The particular ones passing by the neighborhood of the orbit of the Earth are called "Near Earth Asteroids" (NEAs). Among the NEAs, a particular important class is formed by binary and triple systems. The NEAs may contain information that would help to explain the formation of the Solar System. Therefore, many missions are considered for the exploration of these bodies (Belton et al. 1992, 1996; Veverka et al. 2001; Broschart and Scheeres 2005; Huntress et al. 2006; Yoshikawa et al. 2007; Bellerose et al. 2008; Brum et al. 2011; Jones et al. 2011; Surovik and Scheeres 2014; Sukhanov et al. 2010; Aljbaae et al.

Springer

Table 1 Physical data and orbital elements of the system 2002CE$_{26}$ (Johnston 2016)

Asteroid	Main body	a (km)	e	I	Period	Radius (km)	Mass (kg)
Primary	Sun	3.34×10^8	0.56	47.29°	3.34 years	1.73 km	1.95×10^{13}
Secondary	Primary	4.7	0.00	22.5°	0.65 days	0.15 km	1.27×10^{10}

2017). Recently, NASA launched the Osiris-Rex spacecraft, in September 2016, to reach the asteroid Bennu (formerly called 1999RQ$_{36}$) in 2018. The goal is to collect data from this asteroid and return samples to the Earth in 2023. Some other researches, like the ones by Werner (1994), Scheeres (1994, 2012a, 2012b, 2012c), Rossi et al. (1999), Scheeres and Hu (2001), Bartczak et al. (2006), Byram and Scheeres (2009), Prado (2014a, 2014b), Shang et al. (2015), Yang et al. (2015), Zeng et al. (2016), were made considering trajectories around smaller bodies. They have a good potential to be used in missions to asteroids.

The gravitational fields of the asteroids are very weak, due to their small masses. Another important feature is the irregular shape of these bodies. The combination of these two factors generates orbits around the system that are far from Keplerian. It means that predictions based on this simple model, which is usually considered as a first model to study orbits around larger bodies, cannot be used for more than a few hours in the case of asteroids, sometimes even minutes.

There are many researches looking for stable orbits around small and irregular bodies, like the ones by Holman and Wiegert (1999), Hu and Scheeres (2004) and Mudryk and Wu (2006). In particular, Hu and Scheeres (2004) search for stable orbits around a rotating irregular body using a very practical definition of stability. They consider an orbit stable if the eccentricity does not reach a fixed limit. In a highly perturbed environment like a double asteroid with the inclusion of the solar radiation pressure, stable orbits in any sense occur only for short times and for small ranges of initial conditions. For this reason, and to give a different and applied criterion to choose orbits around small bodies, the present paper does not look for stable orbits around one of the asteroids, but searches for orbits that stay for reasonable times near both of the primaries, such that the spacecraft can take measurements of both asteroids from short distances, like done in Masago et al. (2016) for a triple asteroid. In that sense, the present paper shows a different and complementary approach to what is usually done in the literature and the results are not directly comparable to the ones searching for stable orbits. In fact, unstable orbits can be considered interesting for the criterion used here, if the spacecraft changes its proximity from one body to the other. On the other side, stable orbits that stays around one of the primaries and that do not approach the other primary are not interesting in the present criterion, even if they are stable by other definitions.

Considering those facts, this study searches for orbits that make the spacecraft to remain as long as possible near the two asteroids of the system. These orbits may be used as a single piece, or several of those orbits can be combined in a single trajectory by orbital maneuvers. The use of these combinations makes possible to build a trajectory that alternates observations among the two bodies, spending some time near one asteroid and then moving to the other one. It is also important to verify if these trajectories do not make close approaches with one of the bodies, which would change the energy of the spacecraft, in a so-called "Swing-By maneuver" (Broucke 1988; Gomes and Prado 2008; Broucke and Prado 1993). In the case of the occurrence of these close encounters, it is important to verify the possibility of escapes of the spacecraft from the system of asteroids. This verification is done here.

2 The double asteroid 2002CE$_{26}$

The double asteroid 2002CE$_{26}$ was discovered in February 10, 2002, in the city of Socorro, in the American state of New Mexico. It is a result of the project Lincoln Near-Earth Asteroid Research (LINEAR), which is a research project devoted to the observation of the sky to search for unknown bodies. The system consists of two bodies. The central one has a diameter of 3.46 km and the smaller body has 0.30 km in diameter (Johnston 2016). Table 1 shows the physical data observed from the Earth (sizes and masses) and the orbital elements of the bodies. The usual symbols a, e and i are used to represent, respectively, the semi-major axis, eccentricity and inclination of each asteroid. Based on those data, it is possible to calculate the sphere of influence of the asteroid. For this task, the radius of Hill (Araújo et al. 2008) is chosen, which is given by $R_{\text{Hill}} = (\frac{\mu_{\text{ast}}}{3})^{1/3} r_{\text{as}}$, where $\mu_{\text{ast}} = 9.75 \times 10^{-18}$ is the mass parameter of the asteroid system (mass ration asteroid/Sun) and r_{as} is the asteroid-Sun distance, which goes from 1.47×10^8 km to 5.20×10^8 km. Based on those numbers, the sphere of influence of the asteroid system goes from 217 to 770 km.

3 Description

The present paper has three main goals. The first one is to search for orbits around the primary body of the double system of asteroids 2002CE$_{26}$ that can observe both bodies.

They are very important, because orbits around the smaller body are very hard to find, due to its small mass. In this phase, a distance up to 5 km is considered to be good enough to observe the bodies. Therefore, the present research measures the time the spacecraft stays inside this limit from each asteroid. A second goal is to make a general study of the effects of the errors in the physical parameters of the bodies, identifying the orbits that are more or less affected by those errors. The third goal is to find trajectories that have reasonable observation times for both bodies in all the error scenarios simulated. Those orbits are very good candidates to place the spacecraft in when it arrives in the system. At the arrival time, there will be larger uncertainties in the sizes and masses of the bodies. In that way, an initial parking orbit that can observe both bodies, independent of the error scenario assumed, can help the mission. For this goal, even observation distances from 5 to 10 km are useful, since the idea is just to improve the accuracy of the physical data of the bodies and not to make the final observations intended for the mission. From this trajectory the spacecraft can observe the system and get a better estimation of those values, therefore allowing a better choice of the orbits that can be used during the mission.

The model used in the simulations made here considers all the known relevant information as regards the double asteroid system, like their sizes, masses, shapes, etc. The force coming from the solar radiation pressure is also included in the model, because it is an important force in an ambient of weak gravity fields, like the ones existing in a double asteroid system. Based on observations made from the Earth, the semi-major axis, eccentricity and inclination of the bodies are known, but with some errors, which are not negligible. The mathematical model used here assumes Keplerian elliptical orbits for the smaller body of the system around the larger one. The reference system has the origin in the primary body and uses the orbital plane of the smaller body as the reference plane. The gravitational perturbations of the Sun, Moon and the planets Venus, Earth, Mars, Jupiter and Saturn were studied and they revealed to be much smaller than the forces included in the model. The model derived in Masago et al. (2016), used for a similar study in the system 2001SN$_{263}$ (Araújo et al. 2012; Araújo et al. 2015), is not applied in the present study because the effects of the flattening of the central body is not relevant in the present case. It means that the precession of the spacecraft and the smaller body of the asteroid system is not taken into account.

The results obtained in this research indicated the existence of orbits around the main body that are able to observe the two bodies of the system, for all the scenarios of errors simulated. The observation times, defined as the time that the spacecraft remains at a given distance from each body, is measured and used as a criterion to select the best orbits to place the spacecraft, as done in Masago (2014) for the triple asteroid system 2001SN$_{263}$.

Another important point considered here is the accuracy of the physical data. These data are obtained from observations based on the Earth, which introduce errors that can be large in some cases. Therefore, the present paper makes a study of the consequences of those errors in the observation times for each body. It is assumed that the errors in the total mass of the system have the value presented in Johnston (2016), which is 2.5×10^{12} kg. For the radius of the bodies, an error in the order of 10% is assumed for both bodies. Of course this number can be modified and the algorithm used here can be applied to any desired value for this error. In that way, the orbits are simulated for five different scenarios. The first one uses the nominal values for the physical data, which is the case when no errors are introduced. The second one uses the nominal values for the radius, but it considers the radius of the larger body to be 10% larger than the nominal value, while the radius of the smaller body is 10% below the nominal value. The third scenario considers a similar situation, but now the radius of the larger body is 10% below the nominal value and the radius of the smaller body is 10% larger than expected. The next scenario uses the nominal mass ratio, but assumes that the total mass of the system is 2.5×10^{12} kg larger than expected. The last and fifth scenario is similar to the previous one, but the total mass of the system is 2.5×10^{12} kg below the nominal value. The mass ratio of the system is modified in the second and third scenarios, because it is assumed a constant and equal density for both bodies. It means that the masses of the individual bodies are proportional to their volumes, which means that they are proportional to the cube of their radius. So, the mass ratio is a function of the radius of the bodies. Situations were both radius were above or below the nominal values were simulated, keeping the same total mass and modifying the density of the bodies, but the differences, compared to the nominal situation, are very small. This is the reason why the results of this scenario are not shown in the present paper.

The results showed very large differences in terms of trajectories and observational times. It is very important to have choices available for the best orbits to place the spacecraft, such that a final decision can be made when the spacecraft reaches the system and is able to take new data to make a more accurate determination of the physical data from the bodies composing the system.

4 Mathematical models

To reach the goal of this work, it is necessary to define a mathematical model for the dynamics of the system that is not too complex, but that can represent the system with some

accuracy. A reference frame is defined centered in the main body and using a reference plane coincident with the orbital plane of the bodies. The motion of the spacecraft is governed by the gravitational forces of the two bodies and the solar radiation pressure. Since the masses, sizes and shapes of the bodies are not accurately known, it does not make sense to add other perturbations in the system, because they have smaller magnitudes when compared to the effects of the unknown parameters.

The distances between the spacecraft and both bodies of the system are given by Eqs. (1) and (2), where r_1 is the distance between the spacecraft and the central body and r_2 is the distance between the spacecraft and the secondary body. We have

$$r_1 = \sqrt{(x - x_1)^2 + (y - y_1)^2 + (z - z_1)^2}, \tag{1}$$

$$r_2 = \sqrt{(x - x_2)^2 + (y - y_2)^2 + (z - z_2)^2}. \tag{2}$$

These distances are very important when choosing the best trajectories for the spacecraft, because the goal is to search for orbits that keep the spacecraft as long as possible closer to one of the bodies, so having low values for these parameters. The equations of motion, in the inertial system, are represented by Eqs. (3)–(5):

$$\ddot{x} = -\mu_2 \frac{(x - x_2)}{r_1^3} - \mu_1 \frac{(x - x_1)}{r_2^3} + P_{radx}, \tag{3}$$

$$\ddot{y} = -\mu_2 \frac{(y - y_2)}{r_1^3} - \mu_1 \frac{(y - y_1)}{r_2^3} + P_{rady}, \tag{4}$$

$$\ddot{z} = -\mu_2 \frac{(z - z_2)}{r_1^3} - \mu_1 \frac{(z - z_1)}{r_2^3} + P_{radz}, \tag{5}$$

where P_{radx}, P_{rady} and P_{radz} represent the components x, y and z of the acceleration due to the solar radiation pressure; μ_1 and μ_2 are the gravitational parameters of the primary and secondary bodies. The magnitude of the acceleration due to the solar radiation pressure is given by Eq. (6):

$$P = \frac{h(1 + \epsilon)}{c} \frac{S}{m} \left(\frac{r_0}{R} \right)^2 \cos \alpha^2 \tag{6}$$

where S is the area of the spacecraft illuminated by the Sun; h is the solar radiation constant at the Sun–Earth distance (around 1360 [W/m^2]); r_0 is the Sun–Earth distance, R is the Sun–spacecraft distance, ϵ is the coefficient of reflectivity; and α is the angle of the incident light (Fieseler 1988), which is assumed to be zero in all the simulations made in this research. Here, the value used for S/m is 0.01 m^2/kg, in all the simulations made.

A coordinate transformation is made to transform the Keplerian elements of the secondary body to Cartesian coordinates. It is used the method found in Kuga et al. (2012). The goal is to find the Cartesian coordinates x, y and z of the body at a given time. This transformation needs to be done to make the necessary numerical integrations to obtain the orbits of the spacecraft.

5 Results

The first step is the choice of the initial conditions for the orbits of the spacecraft around the main body that allows repeated passages near the secondary body. After finding these orbits, the numerical integration is performed starting at the periapsis and the apoapsis of the orbit. The numerical integrations are made using a fourth-order Runge–Kuta method with variable stepsize. The accuracy used is 10^{-10}. The algorithm also verifies the possibility of collisions at every step of integration. If the distance between the spacecraft and the center of one of the bodies reaches a value smaller than the radius of this body, it is considered that a collision took place and the numerical integration is stopped. This technique avoids situations where one of the spacecraft-asteroid distances is small enough to introduce errors above the limit specified for the numerical integrations, therefore regularization techniques (Prado and Broucke 1995; Prado 2007) are not necessary.

Initially, the orbits are investigated based on the problem of the two bodies (main asteroid-spacecraft). This is done to find initial conditions for the numerical integrations of the orbits. It is searched for orbits with periods that are resonant with the period of the orbit of the secondary body around the primary. It means that those periods can be related by a fraction of two integer numbers. This relation is enough to generate orbits for the spacecraft that has repeated passages by the secondary body of the system, under the two-body dynamics. Of course that these orbits are modified by the more complex dynamical system that includes other forces, but they still have a good potential to allow consecutive passages of the spacecraft by the secondary body. Since this is just a starting point for the search of the orbits, it does not need to be very accurate. The results showed that those initial conditions are good enough to find the desired orbits.

After finding the initial conditions, the orbits are numerically integrated with the force model explained before. The evolution of the distances between the spacecraft and the larger and the smaller asteroid, r_1 and r_2, respectively, are monitored, and the times that the spacecraft remains close to both bodies are computed and showed in the results.

Since the bodies are small, the results show the total time that the spacecraft remains in a distance smaller than 5 km from the center of the asteroids, taking into account that no collisions occur with any of the bodies. This distance is good enough to allow observations with high quality. The intervals of distances from 5 to 10 km are also measured.
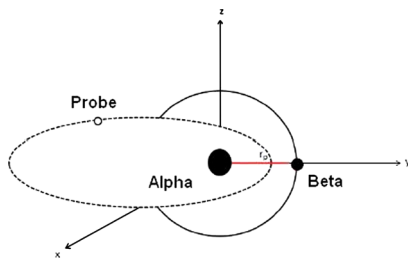
Fig. 1 Initial external orbit

They can be used for some types of observations that can be done far from the body and also as the first parking orbit, before the precise determination of the physical parameters of the bodies are made by the spacecraft. The integrations also detected the occurrence of swing-bys with the secondary body, so orbits that suffer variations of energy that are large enough to make the spacecraft to go far from the system are excluded from the results. Through this criterion, it is possible to choose the most interesting orbits. Five different scenarios are simulated: (i) orbits obtained under the nominal values for the physical parameters, so without errors; (ii) orbits obtained under a model that adds an error of 10% to the radius of the main body (R1) and subtracts 10% of the radius of secondary body (R2), keeping the nominal total mass, which is indicated by "R1+10% and R2-10%"; (iii) orbits obtained when reducing in 10% the radius of the main body (R1) and increasing 10% in the radius of the secondary body (R2), keeping the nominal total mass, which is indicated by "R1-10% and R2+10%"; (iv) orbits obtained when considering an error of 2.5×10^{12} kg (Johnston 2016) is added to the value of the total mass of the bodies, keeping the nominal radius of the bodies, which is indicated by "Mass plus error" and; (v) orbits obtained when an error of 2.5×10^{12} kg is subtracted from the value of the total mass of the bodies, keeping the nominal radius of the bodies, which is indicated by "Mass minus error". All of those scenarios are considered for the situation when the asteroid is at its periapsis (anomaly 0°) and when it is at its apoapsis (anomaly π). It is important to consider those two situations, because the eccentricity of the orbit of the asteroid is large ($e = 0.56$) and the effects of the solar radiation pressure are very different at those two points, due to the different Sun-asteroid distances.

To obtain the resonance condition, the problem must be divided in two cases: (i) initial internal orbits, when the semi-major axis of the spacecraft is smaller than the semi-major axis of the orbit of the secondary body, and; (ii) initial external orbits, when the semi-major axis of the spacecraft is larger than the semi-major axis of the orbit of the secondary body. Figure 1 shows an example of an initial external orbit.

This division is necessary for the correct placement of the terms in Eq. (7), which expresses the resonance condition.

This equation is taken from Murray and Dermott (1999), after making $\dot{\varpi}' = 0$, which means that the time derivative of the longitude of the periapsis of the secondary body ($\dot{\varpi}'$) is neglected in the present case.

$$\frac{p}{p+q} = \frac{n'}{n}. \tag{7}$$

For the internal orbits situation, n is the mean motion of the spacecraft and n' the mean motion of the secondary body. To get a specific resonance condition it is necessary to specify the values of p and q, where p is the number of revolutions of the secondary body and ($p + q$) is the number of revolutions of the spacecraft. For the external orbits situation, n is the mean motion of the secondary body and n' is the mean motion of the spacecraft. The order of the resonance is once again given by p and q, but now p is the number of revolutions of the spacecraft and ($p + q$) is the number of revolutions of the secondary body.

For the numerical simulations made here, the values of p and q are limited to the interval from 1 to 5. This choice is made because higher values would result in orbits with very long periods, which would take longer to get close encounters with the bodies of the system, making them with little practical applications. Besides that, for such longer periods, other perturbations would act in the system, so requiring more complex models to study the problem.

In a first analyses, a study of the eccentricities is performed for all the orbits obtained. Orbits with eccentricity larger than 1.0 are discarded, because they are hyperbolic orbits, so they do not allow repeated passages between the spacecraft and the secondary body. A second analysis is made to verify the distances between the spacecraft and the main body (r_1) and between the spacecraft and the secondary body (r_2), both of them as a function of time.

After choosing the initial resonant orbits around the central body that makes the spacecraft to cross repeated times the orbit of the secondary body, it is verified the occurrence of collisions between the spacecraft and both of the asteroids. Removing those cases, the trajectories are numerically integrated using the dynamical system already explained. The duration of the integrations of each orbit are not always the same, because several orbits run the risk of collision with one of the asteroids. These orbits are not discarded, because the part of the orbit that is far from the collision can be used as a piece of a more complex trajectory, obtained by pasting together several orbits linked by orbital maneuvers. Despite of this explanation, the numerical integration is interrupted at this point, since the rest of the natural trajectory is not of interest.

To avoid a large number of data with very little practical interest, only the most interesting orbits are shown next. The criterion to select the orbits is to choose only the ones where the spacecraft remains at least 10 days near one of the

asteroids of the system in at least one of the scenarios simulated. The results are shown in Table 2. The nomenclature of the scenarios shown in this Table was already explained, but notice that R1 is the radius of the larger asteroid and R2 is the radius of the smaller asteroid. The maximum simulation time is 187.50 days. The full nomenclature of all the orbits simulated is found in Table 3.

Analyzing the orbits shown in Table 2, it is observed that several types of situations occur, depending on the errors in the physical parameters. The first type of orbits of interest is the one that allows good conditions to observe both bodies of the system. They are analyzed first.

5.1 Orbits to observe the system under nominal conditions

Orbits 2 and 3 are the best choices to observe the system, if the values of the physical data are the nominal ones, or very close to them. Orbit 2 is an orbit that starts in an internal resonance 2:3 with the smaller body of the system. Using this orbit when the asteroid is at its periapsis (Table 2), the spacecraft remains 177.18 days near the main body and 99.69 days near the secondary body, which are very good values. Figure 2 shows this trajectory. The Sun is at the right of the trajectory, as marked in the figure. When the asteroid is at its apoapsis, it is noted that there are slight decreases in the observational times. The main body is observed during 151.79 days by the spacecraft and the secondary body is observed for 83.53 days (Table 2). Orbits with this property are very important to observe both bodies from an orbit around the central body. Figure 3 shows this trajectory, for the situation where the asteroid is at its apoapsis. The Sun is at the left of the trajectory, as marked in the figure. It is important to remember that the secondary body is in an orbit with semi-major axis of 4.7 km, which is near the left border of Figs. 2 and 3. It means that the trajectories of the spacecraft shown in both figures have crossing points with the orbit of the secondary body in several places, so close approaches are possible. In fact, it happens in some points, which changes the orbit of the spacecraft more drastically.

Orbit 3 is an orbit that starts in an internal resonance 3:4 with the smaller body of the system. In this orbit, the spacecraft remains 161.92 days observing the main body and 90.95 days next to the secondary body. Those are also good values, equivalent to the ones obtained using Orbit 2. When the asteroid is at its apoapsis, the main body is observed during 159.80 days and the secondary body for 90.25 days.

5.2 Effects of the errors of the physical parameters in the trajectories of the spacecraft

The attention is now turned to the second goal of the paper, which is the analysis of the effects of the errors of the physical parameters on the trajectories of the spacecraft, in the particular aspect of the observational times. To make this study, simulations are made assuming the five scenarios explained before: (i) nominal values; (ii) "R1+10% and R2-10%"; (iii) "R1-10% and R2+10%"; (iv) "mass plus error" and (v) "mass minus error".

After making those simulations, the results are shown in plots that have vertical bars representing the observation times for each scenario. The observational time is the total time the spacecraft spends at a distance below 5 km from each body. The bar at the left side of the pair (marked in blue) gives the results with respect to the main body, while the bar at the right side of the pair (marked in red) represents the results with respect to the secondary body.

The first orbit to be analyzed in this aspect is Orbit 2, which is one of the best orbits to observe the system. Figure 4 shows the results. It is noted there are very strong effects of the errors in the physical data. This orbit is excellent to observe the bodies in the nominal situation, but it does not spend any time at distances below 5 km from any of the bodies in the second scenario "R1+10% and R2-10%". In the error scenarios involving the total mass, the observational times are very small: 1.17 days near the primary body and 0.66 days near the secondary body, in the scenario "Mass plus error"; and 0.34 days near the primary and 0.22 days near the secondary, in the scenario "Mass minus error". The only error scenario that keeps very good observational times is the third scenario, "R1-10% and R2+10%". In this case, the spacecraft remains 176.83 days observing the main body and 95.81 days next to the secondary body, which are very good values.

The same effects are noted when the asteroid is at its apoapsis. Figure 5 shows the results. The same behavior exists, and only the third error scenario "R1-10% and R2+10%" keeps good values for the observational times. The observational times are now 151.79 days for the main body and 83.53 for the secondary body, for the nominal situation; and 157.21 days for the main body and 86.19 for the secondary body, for the third error scenario. The other scenarios have orbits with almost no observation times with respect to both bodies, showing values below 1.17 days.

This is a very good example of the strong effects of the errors in the values of the physical parameters and the importance to study this problem.

The study of Orbit 3 confirms these strong effects. Figure 6 shows the results when the asteroid is at its apoapsis, which is the best case for this orbit. Table 2 shows that this orbit has a similar behavior when the spacecraft is at its periapsis, but the observational times are very small in some scenarios. For the situation of the asteroid near the apoapsis, this orbit is an excellent choice when the physical data are correct, and much better than Orbit 2 when errors are introduced. In the nominal case, the spacecraft spends

Table 2 Orbits with at least 10 days of observation in one of the scenarios

Nominal values			R1+10% and R2-10%		R1-10% and R2+10%		Mass plus error		Mass minus error	
Orbits with the spacecraft starting in the periapsis	True anomaly 0°	True anomaly 180°	True anomaly 0°	True anomaly 180°	True anomaly 0°	True anomaly 180°	True anomaly 0°	True anomaly 180°	True anomaly 0°	True anomaly 180°
2 (I 2:3)										
R_1	177.18	151.79	0	0	176.83	157.21	1.17	1.17	0.34	0.34
R_2	99.69	83.53	0	0	95.81	86.19	0.66	0.67	0.22	0.21
3 (I 3:4)										
R_1	161.92	159.8	171.22	156.08	3.2	15.44	3.11	7.28	9.61	15.55
R_2	90.95	90.25	90.47	90.18	2.09	13.56	1.18	3.49	4.74	7.07
5 (I 4:5)										
R_1	6.32	12.55	25.53	6.84	1.77	1.78	3.22	8.48	145.59	37.03
R_2	2.55	5.74	16.04	5.02	1.03	1.04	1.7	3.78	88.72	20.13
8 (I 5:7)										
R_1	13.95	7.01	8.5	6.18	1.23	1.23	166.3	157.07	177.19	154.08
R_2	7.19	4.42	4.53	3.46	0.7	0.71	92.05	92.68	100.72	83.76
9 (I 5:8)										
R_1	0.32	0.32	0	0	3.22	30.95	177.21	153.17	0	0
R_2	0.2	0.2	0	0	1.57	17.55	91.95	84.85	0	0
11 (E 1:2)										
R_1	6.6	9.3	2.7	1.04	8.84	2.49	0.26	7.53	18.21	42.99
R_2	4.45	9.79	24.52	1.42	12.1	4.31	0.45	10.93	51.45	46.08
12 (E 1:3)										
R_1	3.04	3.22	3.3	17.69	2.08	2.77	1.4	0.24	1.48	4.37
R_2	27.32	5.47	17.27	46.29	4.78	2.7	1.34	0.37	1.1	4.17
13 (E 1:4)										
R_1	2.44	11.94	3.64	10.62	2.33	0.09	2.61	16.62	1.81	5.15
R_2	7.19	17.62	13.96	19.07	10.42	0.34	12.4	13.8	1.54	4.14
14 (E 1:5)										
R_1	3.38	15.09	1.61	4.84	1.4	3.06	1.93	1.82	1.96	5.82
R_2	11.58	14.36	4.93	8.07	3.38	2.36	6.64	1.57	4.78	4.87
17 (E 2:5)										
R_1	5.78	11.32	3.56	2.55	4.38	27.59	3.53	0.42	1.71	9.77
R_2	7.02	10.96	5.35	2.47	4.17	18.86	18.27	0.6	1.6	9.08
18 (E 2:7)										
R_1	1.97	0.98	2.11	13.52	2.29	1.67	1.8	2.71	2.82	4.36
R_2	8.4	0.97	2.34	14.31	2.18	0.86	8.02	3.39	3.41	8.07
19 (E 3:4)										
R_1	9.16	1.94	3.12	20.11	10.45	4.18	5.36	12.27	30.33	3.28
R_2	10.1	1.43	3.44	21.69	7.42	3.31	53.36	16.76	23.24	3.59
21 (E 3:7)										
R_1	2.28	7.11	5.2	8.74	3.69	1.83	3.53	12.97	4.22	0.73
R_2	3.28	6.73	6.06	8.88	3.94	1.67	3.71	12.75	4.31	0.72
22 (E 3:8)										
R_1	3.39	1.02	2.29	5.6	2.82	0.48	5.55	15.08	1.74	17.14
R_2	3.68	2.33	10.95	5.36	23.25	0.88	4.59	13.92	2.17	19.83
23 (E 4:5)										
R_1	21.77	40.17	9.79	3.01	3.21	29.63	4.67	10.53	2.6	5.78
R_2	21.83	25.84	10.49	3.23	3.6	32.03	3.88	7.86	2.36	3.59

Table 2   (*Continued*)

Nominal values			R1+10% and R2-10%		R1-10% and R2+10%		Mass plus error		Mass minus error	
Orbits with the spacecraft starting in the periapsis	True anomaly 0°	True anomaly 180°	True anomaly 0°	True anomaly 180°	True anomaly 0°	True anomaly 180°	True anomaly 0°	True anomaly 180°	True anomaly 0°	True anomaly 180°
24 (E 4:7)										
R_1	26.52	1.91	8.25	8.55	2.57	26.55	38.94	7.33	1.52	4.82
R_2	50.07	1.62	44.76	9.06	2.68	24.01	25.61	7.41	2.14	6.48
25 (E 4:9)										
R_1	5.82	3.61	4.1	6.4	0.69	1.44	5.05	13.76	18.08	7.14
R_2	20.1	3.49	3.92	8.35	0.61	1.55	12.8	13.93	20.9	14.27
26 (E 5:6)										
R_1	8.93	13.83	1.25	6.14	4.87	24.06	7.21	1.34	4.15	5.43
R_2	9.25	14.43	0.9	6.84	4.56	21.32	8.5	1.45	6.39	7.16
27 (E 5:7)										
R_1	5.72	0.81	9.34	24.47	16.09	8.05	1.2	1.55	8.14	0.98
R_2	7.35	0.89	10.34	27.71	11.58	7.78	1.36	2.72	6.39	0.67
28 (E 5:8)										
R_1	3.06	13.73	5.94	5.06	2.89	11.34	11.27	36.75	3.12	12.54
R_2	4.08	14.35	7.14	6.66	5.71	19.57	15.38	37.04	3.45	17.18
29 (E 5:9)										
R_1	3.18	7.48	2.96	20.62	1.49	0.72	3.53	1.69	12.69	0.59
R_2	3.04	8.93	3.08	21.45	6.29	0.77	4.1	1.95	12.7	0.51
Orbits with the spacecraft starting in the apoapsis										
31 (I 2:3)										
R_1	2.69	10.75	0.14	0.14	3.6	3.48	7.22	2.31	13.19	6.35
R_2	1.22	5.83	0.2	0.2	3.05	2.14	2.97	1.03	7.62	3.37
32 (I 3:4)										
R_1	1.63	18.21	3.81	21.12	8.67	2.65	13.2	10.27	9.08	20.44
R_2	1.32	10.85	1.97	9.5	4.57	1.59	6.96	5.74	4.66	12.62
34 (I 4:5)										
R_1	11.83	14.26	6.9	34.41	4.83	18.74	5.4	4.06	6.19	1.38
R_2	6.82	8.17	3.67	19.11	2.58	10.02	3.16	1.98	4.67	0.52
36 (I 5:6)										
R_1	4.9	18.41	7.73	17.38	8.6	4.89	2.54	10.94	2.57	7.48
R_2	2.69	11.77	4.45	9.84	5.22	3.01	1.76	12.4	1.56	3.28
37 (I 5:7)										
R_1	1.41	12.19	13.06	16.06	1.38	2.71	13.08	121.89	1.14	7.95
R_2	0.74	5.02	7.11	8.32	0.43	0.97	8.54	74.84	0.69	4.01
38 (I 5:8)										
R_1	2.62	6.11	0.15	0.15	56.06	5.32	4.36	10.37	0.14	0.14
R_2	1.19	2.94	0.19	0.19	51.34	2.67	2.29	5.09	0.18	0.18
40 (E 1:2)										
R_1	6.67	28.65	5.96	28.65	7.73	28.71	1.89	8.47	0.85	2.64
R_2	0	0	0	0	0	0	0.79	7.12	0.71	2.43
41 (E 1:3)										
R_1	2.21	17.56	2.05	14.3	2.22	13.22	2.47	12.49	1.8	10.59
R_2	5.04	48.92	4.84	34.17	4.98	36.68	2.39	12.01	1.32	7.15

Table 2 (*Continued*)

Nominal values			R1+10% and R2-10%		R1-10% and R2+10%		Mass plus error		Mass minus error	
Orbits with the spacecraft starting in the apoapsis	True anomaly 0°	True anomaly 180°	True anomaly 0°	True anomaly 180°	True anomaly 0°	True anomaly 180°	True anomaly 0°	True anomaly 180°	True anomaly 0°	True anomaly 180°
45 (E 2:3)										
R$_1$	13.16	42.77	11.06	42.68	15.34	42.82	5.89	6.19	10.05	4.4
R$_2$	10.05	28.59	8.01	27.93	12.37	29.77	5.69	7.53	10.73	4.27
46 (E 2:5)										
R$_1$	3.81	21.22	3.62	21.38	4.31	15.24	4.47	1.41	3.7	23.73
R$_2$	2.36	13.72	2.06	13.55	3.07	9.1	3.79	1.9	3.61	23.18
48 (E 3:4)										
R$_1$	16.53	30.2	9.98	50.27	17.72	5.09	14.84	4.44	1.92	17.44
R$_2$	16.25	33.7	10.32	53.22	13.28	5.98	11.14	4.3	2.31	12.66
49 (E 3:5)										
R$_1$	3.87	1.97	9.49	19.59	5.41	4.3	1.76	4.55	6.18	11.52
R$_2$	4.02	2.85	10.26	25.56	6.35	6.24	2.06	5.04	6.76	11.85
50 (E 3:7)										
R$_1$	4.03	23.9	3.67	23.62	5.07	5.68	3.93	16.1	2.68	2.47
R$_2$	3.91	22.64	3.39	24.11	4.17	5.56	2.23	9.17	1.81	2.22
51 (E 3:8)										
R$_1$	0.53	5.59	1.29	9.14	5.63	10.72	2.09	0.86	3.67	21.41
R$_2$	0.56	5.44	1.48	8.61	3.9	18.33	1.75	0.59	2.13	13.05
52 (E 4:5)										
R$_1$	47.37	10.52	23.66	4.39	4.78	7.2	9.84	38.57	5.34	24.81
R$_2$	50.36	10.89	25.84	4.35	4.7	12.98	10.7	41.94	6.2	25.54
54 (E 4:9)										
R$_1$	4.17	2.34	4.18	15.95	4.8	7.51	4.18	1.36	4	15.27
R$_2$	3.74	2.28	4.89	13.97	5.19	6.76	3.52	1.77	1.84	8.26
55 (E 5:6)										
R$_1$	1.81	3.03	47.94	3.76	4.43	6.39	4.74	8.16	32.98	31.43
R$_2$	2.14	4.65	49.74	3.37	4.42	6.22	5.3	9.43	36.47	26.88
56 (E 5:7)										
R$_1$	13.49	8.52	11.26	48.21	12.37	3.98	14.57	42.81	13.22	27.66
R$_2$	13.98	10.24	11.87	52.55	11.37	4.19	11.38	29.61	13.69	31.29
57 (E 5:8)										
R$_1$	6.65	3.75	12.24	3.71	3.3	6.82	7.92	19.54	11.24	42.67
R$_2$	7.27	6.44	13.21	4.56	3.5	8.01	7.51	21.11	8.5	28.46
58 (E 5:9)										
R$_1$	6.11	2.86	6.35	33.27	6.51	12.65	7.53	27.71	6.67	35.42
R$_2$	5.21	2.84	6.17	30.77	5.91	13.98	4.6	12.79	6.53	35.35

159.80 days close to the main body and 90.25 days close to the second body. The results are also very good in the second scenario "R1+10% and R2-10%" and the spacecraft spends 156.08 days close to the main body and 90.18 days close to the secondary body. The observation times are much smaller in the third scenario "R1-10% and R2+10%", but they are still reasonable, and the spacecraft spends 15.44 days close to the main body and 13.56 days close to the secondary body. In the error scenarios involving the total mass, the observational times are small, but not zero, as occurred in several other cases: 7.28 days observing the primary and 3.49 days observing the secondary body, in the scenario "Mass plus error", and 15.55 days observing the primary and 7.07 days observing the secondary body, in the scenario "Mass minus error". This combination of results

Table 3 Nomenclature of the orbits

Orbit	Orbits with the spacecraft starting in the periapsis	Orbit	Orbits with the spacecraft starting in the apoapsis
1 (I 1:2)	Internal orbit in resonance 1:2	30 (I 1:2)	Internal orbit in resonance 1:2
2 (I 2:3)	Internal orbit in resonance 2:3	31 (I 2:3)	Internal orbit in resonance 2:3
3 (I 3:4)	Internal orbit in resonance 3:4	32 (I 3:4)	Internal orbit in resonance 3:4
4 (I 3:5)	Internal orbit in resonance 3:5	33 (I 3:5)	Internal orbit in resonance 3:5
5 (I 4:5)	Internal orbit in resonance 4:5	34 (I 4:5)	Internal orbit in resonance 4:5
6 (I 4:7)	Internal orbit in resonance 4:7	35 (I 4:7)	Internal orbit in resonance 4:7
7 (I 5:6)	Internal orbit in resonance 5:6	36 (I 5:6)	Internal orbit in resonance 5:6
8 (I 5:7)	Internal orbit in resonance 5:7	37 (I 5:7)	Internal orbit in resonance 5:7
9 (I 5:8)	Internal orbit in resonance 5:8	38 (I 5:8)	Internal orbit in resonance 5:8
10 (I 5:9)	Internal orbit in resonance 5:9	39 (I 5:9)	Internal orbit in resonance 5:9
11 (E 2:1)	External orbit in resonance 2:1	40 (E 2:1)	External orbit in resonance 2:1
12 (E 3:1)	External orbit in resonance 3:1	41 (E 3:1)	External orbit in resonance 3:1
13 (E 4:1)	External orbit in resonance 4:1	42 (E 4:1)	External orbit in resonance 4:1
14 (E 5:1)	External orbit in resonance 5:1	43 (E 5:1)	External orbit in resonance 5:1
15 (E 6:1)	External orbit in resonance 6:1	44 (E 6:1)	External orbit in resonance 6:1
16 (E 3:2)	External orbit in resonance 3:2	45 (E 3:2)	External orbit in resonance 3:2
17 (E 5:2)	External orbit in resonance 5:2	46 (E 5:2)	External orbit in resonance 5:2
18 (E 7:2)	External orbit in resonance 7:2	47 (E 7:2)	External orbit in resonance 7:2
19 (E 4:3)	External orbit in resonance 4:3	48 (E 4:3)	External orbit in resonance 4:3
20 (E 5:3)	External orbit in resonance 5:3	49 (E 5:3)	External orbit in resonance 5:3
21 (E 7:3)	External orbit in resonance 7:3	50 (E 7:3)	External orbit in resonance 7:3
22 (E 8:3)	External orbit in resonance 8:3	51 (E 8:3)	External orbit in resonance 8:3
23 (E 5:4)	External orbit in resonance 5:4	52 (E 5:4)	External orbit in resonance 5:4
24 (E 7:4)	External orbit in resonance 7:4	53 (E 7:4)	External orbit in resonance 7:4
25 (E 9:4)	External orbit in resonance 9:4	54 (E 9:4)	External orbit in resonance 9:4
26 (E 6:5)	External orbit in resonance 6:5	55 (E 6:5)	External orbit in resonance 6:5
27 (E 7:5)	External orbit in resonance 7:5	56 (E 7:5)	External orbit in resonance 7:5
28 (E 8:5)	External orbit in resonance 8:5	57 (E 8:5)	External orbit in resonance 8:5
29 (E 9:5)	External orbit in resonance 9:5	58 (E 9:5)	External orbit in resonance 9:5
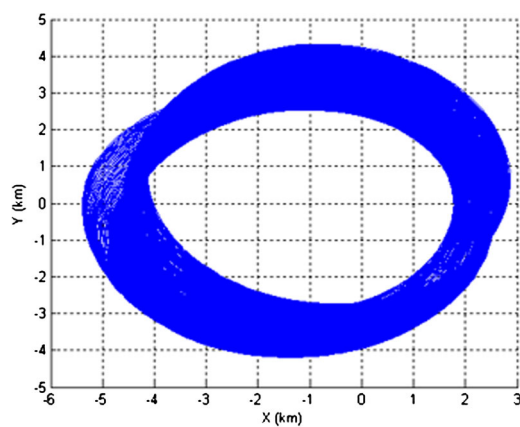
Fig. 2 Orbit 2: spacecraft in the resonance 2:3 (asteroid at periapsis)
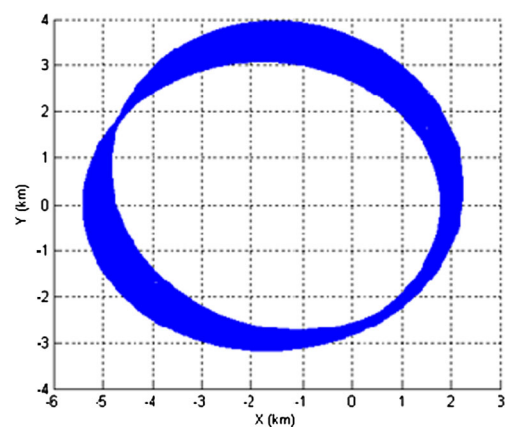
Fig. 3 Orbit 2: spacecraft in the resonance 2:3 (asteroid at apoapsis)

makes of Orbit 3 an excellent choice to place the spacecraft when arriving at the system.

Another interesting option is Orbit 8. When the asteroid is at its periapsis (Fig. 7), the spacecraft remains 166.30
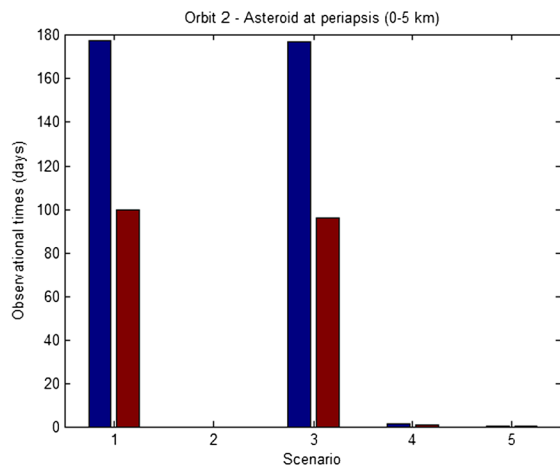
Fig. 4 Observation times of the main (*blue*) and secondary (*red*) bodies for orbit 2 when the asteroid is at its periapsis for the five scenarios simulated: (1) Nominal values, (2) R1+10% and R2-10%, (3) R1-10% and R2+10%, (4) mass plus error and (5) mass minus error
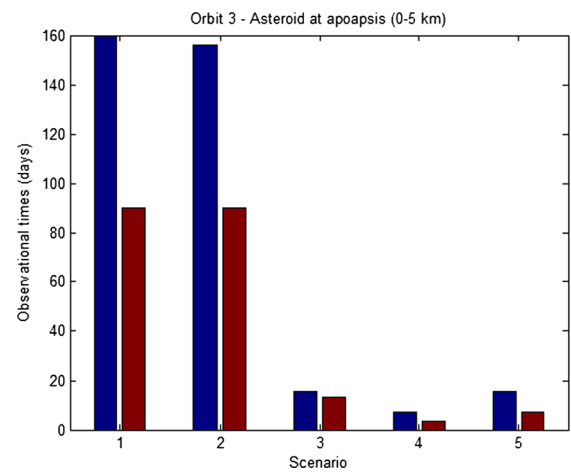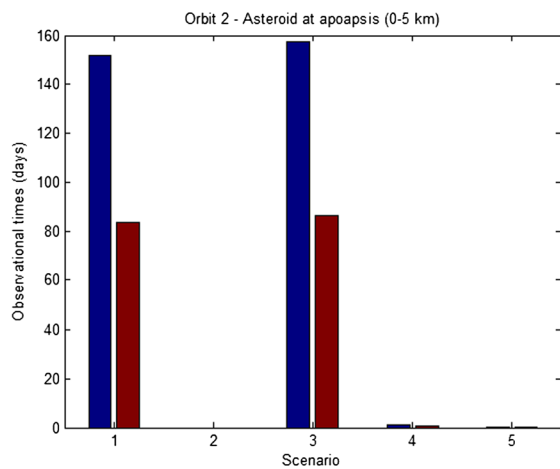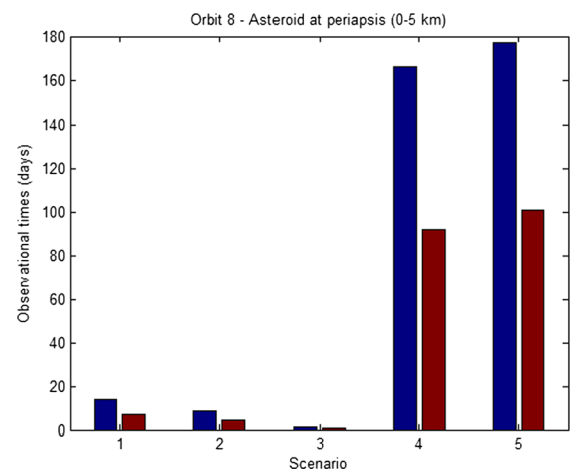

Fig. 6 Observation times of the main (*blue*) and secondary (*red*) bodies for orbit 3 when the asteroid is at its apoapsis for the five scenarios simulated: (1) Nominal values, (2) R1+10% and R2-10%, (3) R1-10% and R2+10%, (4) mass plus error and (5) mass minus error

Fig. 5 Observation times of the main (*blue*) and secondary (*red*) bodies for orbit 2 when the asteroid is at its apoapsis for the five scenarios simulated: (1) Nominal values, (2) R1+10% and R2-10%, (3) R1-10% and R2+10%, (4) mass plus error and (5) mass minus error

Fig. 7 Observation times of the main (*blue*) and secondary (*red*) bodies for orbit 8 when the asteroid is at its periapsis for the five scenarios simulated: (1) Nominal values, (2) R1+10% and R2-10%, (3) R1-10% and R2+10%, (4) mass plus error and (5) mass minus error

days watching the main body in the scenario "Mass plus error" and 177.19 days in the scenario "Mass minus error". The same happens when observing the secondary body, with a time of 92.05 days in the scenario "Mass plus error" and 100.72 days in the scenario "Mass minus error". The same behavior occurs when the asteroid is at its apoapsis. The main body is observed during 157.07 days and the secondary for 92.68 days, in the case "Mass plus error". In the "Mass minus error" scenario, the main body is observed during 154.08 days and the secondary for 83.76 days. Figure 8 shows those results.

It is visible from all the orbits that, in general, the results are very different for each scenario. The best orbits to observe the bodies under nominal conditions are more affected by the variation of the physical parameters. This is expected,

since the spacecraft stays more time closer to the bodies in these orbits, which means that the trajectories of the spacecraft are more affected by the variations of the physical parameters. Orbits with smaller observation times are less affected by the errors, since they travel far away from the primaries. Orbit 21, shown in Figs. 9 and 10, is a good example. The observational times go from 2.28 to 5.20 days to study the main body and from 3.28 to 6.06 days to observe the second body, in the case where the asteroid is at its periapsis. For the case where the asteroid is at its apoapsis, the equivalent numbers go from 0.73 to 12.97 days to study the main body and from 0.72 to 12.75 days to observe the second body. Some other good examples exist, like Orbits 46, 47, 50, 54 and 56.
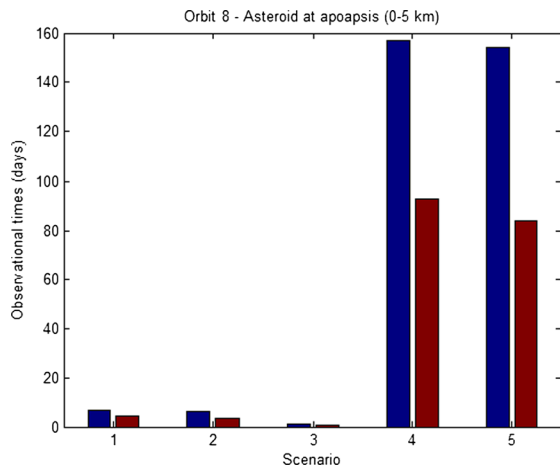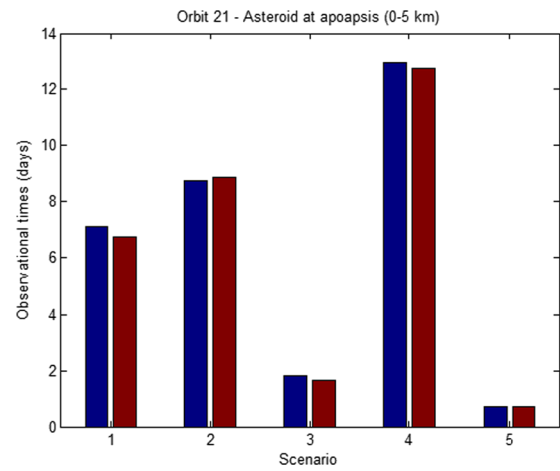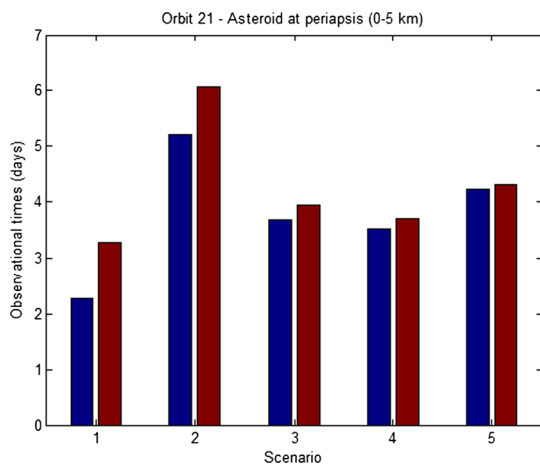
Fig. 8 Observation times of the main (*blue*) and secondary (*red*) bodies for orbit 8 when the asteroid is at its apoapsis for the five scenarios simulated: (1) Nominal values, (2) R1+10% and R2-10%, (3) R1-10% and R2+10%, (4) mass plus error and (5) mass minus error
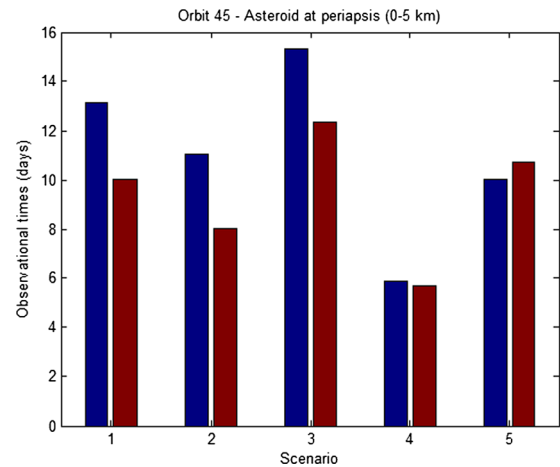
Fig. 10 Observation times of the main (*blue*) and secondary (*red*) bodies for orbit 21 when the asteroid is at its apoapsis for the five scenarios simulated: (1) Nominal values, (2) R1+10% and R2-10%, (3) R1-10% and R2+10%, (4) mass plus error and (5) mass minus error

Fig. 9 Observation times of the main (*blue*) and secondary (*red*) bodies for orbit 21 when the asteroid is at its periapsis for the five scenarios simulated: (1) Nominal values, (2) R1+10% and R2-10%, (3) R1-10% and R2+10%, (4) mass plus error and (5) mass minus error

Fig. 11 Observation times of the main (*blue*) and secondary (*red*) bodies for orbit 45 when the asteroid is at its periapsis for the five scenarios simulated: (1) Nominal values, (2) R1+10% and R2-10%, (3) R1-10% and R2+10%, (4) mass plus error and (5) mass minus error

5.3 Candidates for initial orbit

The next goal is to identify orbits with reasonable observational times in all the error scenarios assumed here. They can be used as initial parking orbits for the spacecraft. From these more stable orbits, with respect to the effects of the errors in the physical parameters in the observational times, the spacecraft can take measurements from both bodies, so making a more accurate estimate of the masses and radius of the bodies. Based on that better information, it is possible to select the most adequate orbits to place the spacecraft. Some of the best examples are Orbits 45, 56 and 58, in particular considering the situation where the asteroid is at its periapsis. Figure 11 is made considering an interval of distances up to 5 km to observe the bodies, while Fig. 12 is

made considering an interval of distances from 5 to 10 km, both for Orbit 45. They show plots indicating the observational times. In the nominal scenario, the spacecraft spends 13.16 days close to the main body and 10.05 days around the second body. The results are also good in the second scenario "R1+10% and R2-10%", and the spacecraft spends 11.06 days close to the main body and 8.01 days around the smaller asteroid. The observation times are better in the third scenario "R1-10% and R2+10%", with the spacecraft spending 15.34 days close to the main body and 12.37 days close to the secondary body. In the error scenarios involving the total mass, the observational times are about the same of the other cases: 5.89 days near the primary and 5.69 near the secondary body, in the "Mass plus error" scenario. For the "Mass minus error" scenario, the equivalent times are 10.05
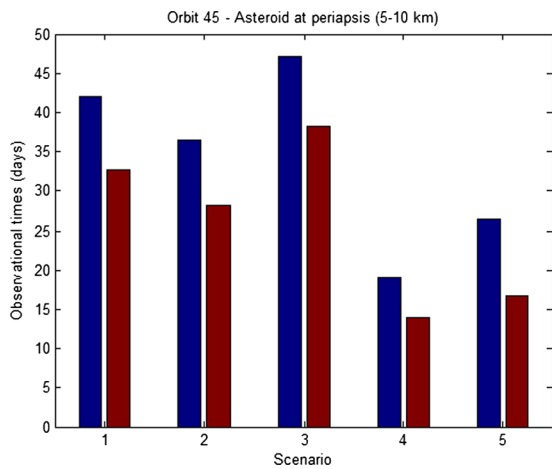
Fig. 12 Observation times of the main (*blue*) and secondary (*red*) bodies for orbit 45 when the asteroid is at its periapsis for the five scenarios simulated: (1) Nominal values, (2) R1+10% and R2-10%, (3) R1-10% and R2+10%, (4) mass plus error and (5) mass minus error

Fig. 13 Observation times of the main (*blue*) and secondary (*red*) bodies for orbit 56 when the asteroid is at its periapsis for the five scenarios simulated: (1) Nominal values, (2) R1+10% and R2-10%, (3) R1-10% and R2+10%, (4) mass plus error and (5) mass minus error

days observing the primary and 10.73 days observing the secondary body. This combination of results makes of Orbit 45 a good choice to place the spacecraft when arriving at the system.

Even better results are available when considering a large interval for the observations. Figure 12 shows the results considering distances from 5 to 10 km, which is also a good interval for the initial parking orbit. For those larger distances, in the nominal case, the spacecraft spends 42.04 days close to the main body and 32.72 days close to the second body. The results are also good in the second scenario "R1+10% and R2-10%", and the spacecraft spends 36.43 days close to the main body and 28.33 days around the secondary body. The observation times are better in the third scenario "R1-10% and R2+10%", and the spacecraft spends 47.14 days close to the main body and 38.29 days close to the secondary body. In the error scenarios involving the total mass, the observational times are smaller, but still acceptable: 19.02 days observing the primary and 13.97 days observing the smaller body, in the "Mass plus error" scenario. For the "Mass minus error" scenario, the times are 26.48 days for the primary and 16.79 days for the secondary body.

Orbit 56 is also a very good choice for an initial orbit. Figure 13 shows the details. It is visible that the observation times go from 11.26 days to 14.57 days with respect to the main body and from 11.37 days to 13.98 days for the secondary body. It is a very equilibrated distribution of times, allowing enough time for the spacecraft to make first observations of both bodies to get a more accurate determination of the physical data.

Figure 14 shows the equivalent results for the distances from 5 to 10 km. The observation times go from 33.32 days to 46.44 days with respect to the main body and from 20.92
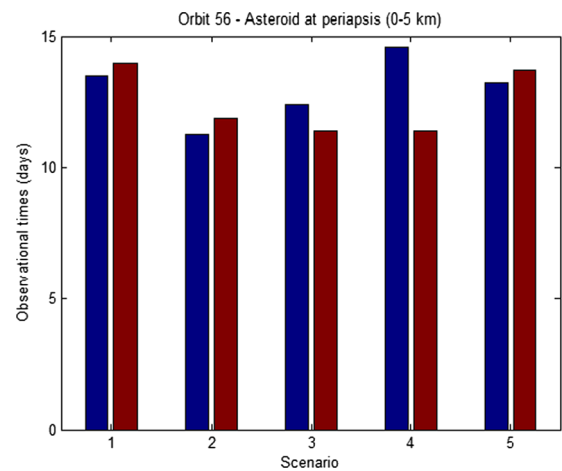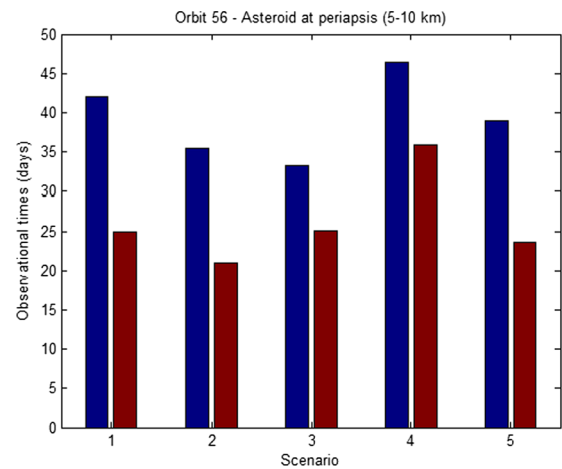

Fig. 14 Observation times of the main (*blue*) and secondary (*red*) bodies for orbit 56 when the asteroid is at its periapsis for the five scenarios simulated: (1) Nominal values, (2) R1+10% and R2-10%, (3) R1-10% and R2+10%, (4) mass plus error and (5) mass minus error

days to 35.91 days for the secondary body. It is also an equilibrated distribution of times, giving some extra time for the spacecraft to make first observations of the bodies and to improve the accuracy of the determination of the physical data.

Some other examples exist, like Orbit 58, but with smaller observational times. Those orbits are very good to observe the bodies when the asteroid is at its periapsis.

When considering the asteroid at its apoapsis, some of the best examples are orbits 3, 36 and 45. Orbit 3 was already described. Orbit 36 is shown in Fig. 15. The observation times go from 4.89 days to 18.41 days with respect to the main body and from 3.01 days to 12.40 days for the secondary body. Figure 16 shows the equivalent results for the interval of distances from 5 to 10 km. The observation times
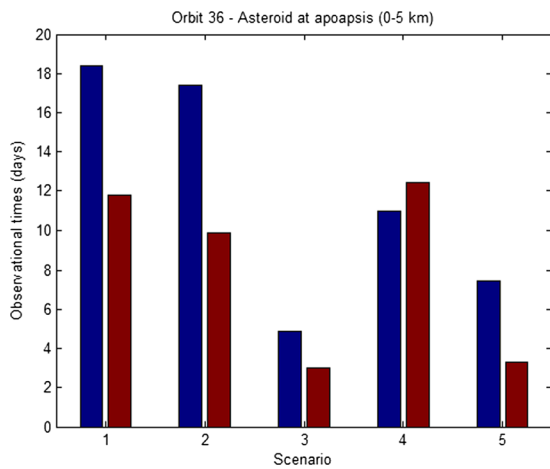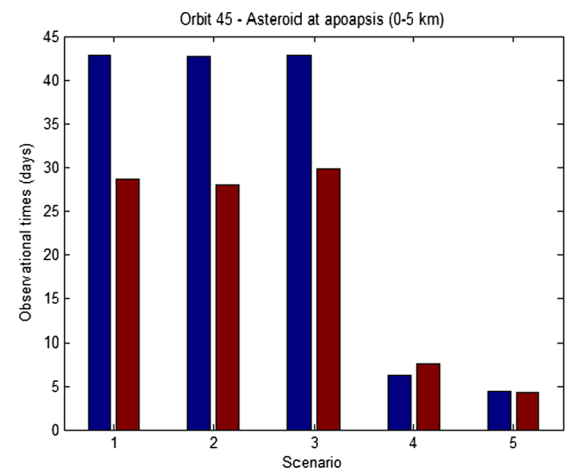
Fig. 15 Observation times of the main (*blue*) and secondary (*red*) bodies for orbit 36 when the asteroid is at its apoapsis for the five scenarios simulated: (1) Nominal values, (2) R1+10% and R2-10%, (3) R1-10% and R2+10%, (4) mass plus error and (5) mass minus error
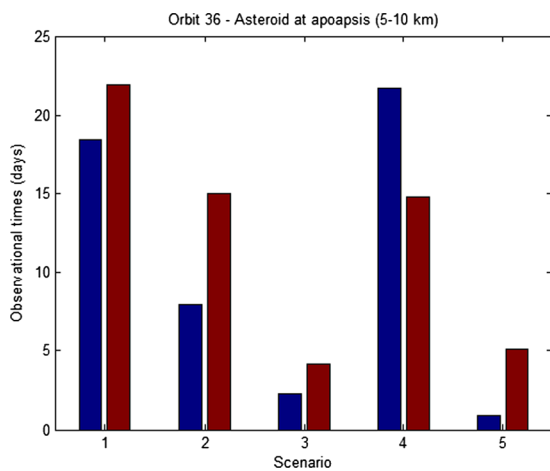

Fig. 17 Observation times of the main (*blue*) and secondary (*red*) bodies for orbit 45 when the asteroid is at its apoapsis for the five scenarios simulated: (1) Nominal values, (2) R1+10% and R2-10%, (3) R1-10% and R2+10%, (4) mass plus error and (5) mass minus error
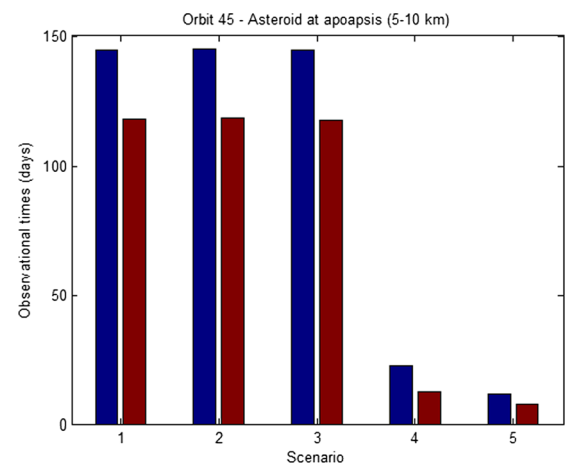

Fig. 16 Observation times of the main (*blue*) and secondary (*red*) bodies for orbit 36 when the asteroid is at its apoapsis for the five scenarios simulated: (1) Nominal values, (2) R1+10% and R2-10% and (3) R1-10% and R2+10%, (4) mass plus error and (5) mass minus error

Fig. 18 Observation times of the main (*blue*) and secondary (*red*) bodies for orbit 45 when the asteroid is at its apoapsis for the five scenarios simulated: (1) Nominal values, (2) R1+10% and R2-10%, (3) R1-10% and R2+10%, (4) mass plus error and (5) mass minus error

go from 0.91 days to 21.77 days with respect to the main body, and from 4.12 days to 21.95 days for the secondary body.

Orbit 45 is even better, and it is shown in Fig. 17. The observation times go from 4.40 days to 42.82 days with respect to the main body. An important aspect of this orbit is that it has very good values, above 42 days, for the first three scenarios, which includes the important case of nominal values, as well as the two scenarios with errors in the sizes of the bodies. With respect to the secondary body, the observation times go from 4.27 days to 29.77 days, with similar good values for the three scenarios, always above 27 days.

The extended regions of Orbit 45, including the interval from 5 to 10 km, also show very good values, which are shown in Fig. 18. The observation times go from 11.69

days to 144.82 days with respect to the main body, keeping the important aspect of showing very good values, above 144 days, for the first three scenarios. With respect to the secondary body, the observation times go from 7.73 days to 118.53 days, with similar very good values for the first three scenarios, always above 117 days.

Those orbits have a small sensitivity to the errors of the physical data and can be used as initial parking orbits for the spacecraft. From those more stable orbits, with respect to the observational times, the spacecraft can take measurements from both bodies, so making a better estimate of the masses and radius of the bodies. After that, it is possible to select other orbits to place the spacecraft. It means that, for the initial orbit, it is interesting to choose the ones that

have smaller observational times in the nominal situation, but preserves good values in all the error scenarios.

6 "Quasi-stable" orbits

A summary of the behavior of the orbits can be made now, studying in more detail the destiny of each orbit. The first point considered here is related to the physical possibility of the initial conditions. The initial conditions are obtained from the resonance condition, as already explained, without taking into account the sizes of the bodies involved. A consequence of this fact is the existence of initial conditions that are located inside one of the bodies, so they are physically impossible initial conditions. They are shown in Table 4. Those orbits are eliminated from future studies.

The next step is to consider which orbits are potential candidates to be used by a spacecraft to observe the bodies

of the double asteroid system. To perform this task, a new definition of "stability of orbits" is made, adequate for the purpose of the present study. This idea is similar to what was done in Hu and Scheeres (2004) that made a practical definition of stability for the purpose of their study. In the present paper, we define the term "quasi-stable" orbits to be applied to orbits that do not collide with one of the primaries and that stays at a distance smaller than 15 km from at least one of the bodies, for a given time. This time is 187.5 days in the present research. Table 5 shows those orbits. "Quasi satellite" orbits are in a small number (31), compared to the total number of orbits studied (580). Tables 6, 7 and 8 show the destiny of the physically possible, but non-"quasi-stable orbits", indicating collisions with one of the bodies of the system and the "Escape orbits", which are the ones that reached 15 km from both bodies, which means more than three times the orbit of the secondary body around the primary. It is observed that the majority of the orbits end in collisions with the secondary body, but escapes and collisions with the primary body also exist. These results identify perfectly the best orbits that are available for a spacecraft willing to observe the system 2002CE$_{26}$.

7 Conclusions

The present paper searches for trajectories for a spacecraft that can be used to observe both bodies of the double asteroid system 2002CE$_{26}$. The idea is to place the spacecraft around the main body, but in conditions to observe both bodies from this orbit. The particular aspect of the evolution of the distances between the spacecraft and the two bodies that compose the system is measured, because it has important impacts in the quality of the observations. In this way, these times are used as the criterion to select the best orbits. The results showed the existence of several orbits with large observational times for both bodies. Some good examples are Orbits 2 and 3, with observation times above 150 days for the nominal values of the physical parameters of the bodies, from the 187.5 days of simulation.

Table 4 Physically impossible orbits

Scenario	Physically impossible orbits	
	Anomaly 0°	Anomaly 180°
Nominal values	1, 4, 6, 10	1, 4, 6, 10
Mass plus error	1, 6, 10	1, 6, 10
Mass minus error	1, 4, 6, 9, 10	1, 4, 6, 10
R1+10% and R2-10%	1, 4, 6, 10	1, 4, 6, 10
R1-10% and R2+10%	1, 4, 6, 10	1, 4, 6, 10

Table 5 Quasi-stable orbits

Scenario	Quasi-stable orbits	
	Anomaly 0°	Anomaly 180°
Nominal values	2, 3, 52	2, 3, 40, 45
Mass plus error	8, 9, 19	8, 9, 37, 56
Mass minus error	5, 8	8, 57
R1+10% and R2-10%	2, 3, 24, 55	2, 3, 40, 45
R1-10% and R2+10%	2, 38	2, 40, 45

Table 6 Orbits that collide with the central body

Scenario	Orbits that collide with the central body	
	Anomaly 0°	Anomaly 180°
Nominal values	9, 30, 33, 35, 39, 40, 41, 42, 43, 44, 45, 46, 47, 50, 56, 58	9, 30, 31, 33, 35, 39, 42, 43, 44, 47
Mass plus error	4, 30, 31, 35, 38, 39, 41, 42, 43, 44, 46, 47, 48, 50, 51, 54, 56, 57, 58	4, 30, 35, 39, 47
Mass minus error	2, 30, 31, 32, 33, 35, 37, 38, 39, 41, 42, 43, 44, 45, 46, 51, 57, 58	2, 9, 30, 33, 35, 37, 38, 39, 41, 44
R1+10% and R2-10%	9, 30, 31, 32, 33, 35, 38, 39, 40, 41, 42, 43, 44, 45, 46, 47, 49, 50, 54, 56, 57, 58	8, 9, 30, 31, 33, 35, 38, 39, 41, 42, 43, 44, 47
R1-10% and R2+10%	30, 33, 35, 39, 40, 41, 42, 43, 44, 45, 46, 47, 48, 50, 51	30, 33, 35, 39, 42, 44

Table 7 Orbits that collide with the secondary body

Scenario	Orbits that collide with the secondary body	
	Anomaly 0°	Anomaly 180°
Nominal values	5, 7, 8, 11, 16, 17, 19, 20, 21, 22, 26, 27, 28, 29, 31, 32, 34, 36, 37, 38, 48, 49, 51, 53, 54, 55, 57	5, 7, 8, 11, 12, 15, 16, 17, 18, 19, 20, 21, 22, 23, 24, 25, 26, 27, 28, 29, 32, 34, 36, 37, 38, 48, 49, 51, 52, 53, 54, 55, 56, 57, 58
Mass plus error	2, 3, 5, 7, 11, 12, 16, 20, 21, 22, 23, 24, 26, 27, 28, 29, 32, 33, 34, 36, 37, 40, 45, 49, 52, 53, 55	2, 3, 5, 7, 11, 12, 14, 15, 16, 17, 18, 19, 20, 21, 22, 23, 24, 25, 26, 27, 29, 31, 32, 33, 34, 36, 38, 40, 41, 42, 43, 44, 45, 46, 48, 49, 50, 51, 52, 53, 54, 55, 57, 58
Mass minus error	3, 7, 12, 13, 16, 17, 18, 19, 21, 22, 23, 24, 25, 26, 27, 28, 29, 34, 36, 40, 47, 48, 49, 50, 52, 53, 54, 55, 56	3, 5, 7, 12, 13, 14, 15, 16, 17, 19, 20, 21, 22, 23, 24, 25, 26, 27, 28, 29, 31, 32, 34, 36, 40, 42, 43, 45, 47, 48, 49, 50, 52, 53, 54, 55, 56, 58
R1+10% and R2-10%	5, 7, 8, 16, 17, 18, 19, 21, 23, 25, 26, 27, 28, 29, 34, 36, 37, 48, 51, 52, 53	5, 7, 11, 13, 14, 16, 17, 19, 20, 21, 22, 23, 24, 25, 26, 27, 28, 29, 32, 34, 36, 37, 49, 51, 52, 53, 54, 55, 57
R1-10% and R2+10%	3, 5, 7, 8, 9, 11, 14, 15, 16, 17, 18, 19, 20, 21, 23, 24, 25, 26, 27, 28, 31, 32, 34, 36, 37, 49, 52, 54, 55, 56, 57, 58	3, 5, 7, 8, 9, 12, 13, 14, 15, 16, 18, 19, 20, 21, 22, 23, 25, 26, 27, 28, 29, 31, 32, 34, 36, 37, 38, 41, 46, 47, 48, 49, 50, 53, 54, 55, 56, 57, 58

Table 8 Escape orbits

Scenario	Escape orbits	
	Anomaly 0°	Anomaly 180°
Nominal values	12, 13, 14, 15, 18, 23, 24, 25	13, 14, 41, 46, 50
Mass plus error	13, 14, 15, 17, 18, 25	13, 28
Mass minus error	11, 14, 15, 20	11, 18, 46, 51
R1+10% and R2-10%	11, 12, 13, 14, 15, 20, 22	12, 15, 18, 46, 48, 50, 58
R1-10% and R2+10%	12, 13, 22, 29	11, 17, 24, 43, 51, 52

After that, the effects of the errors in the physical data of the bodies in the trajectories are studied. It is shown that they are strong enough to destroy the good characteristics even of the best trajectories, depending on the scenario of errors used. Orbits 2 and 3 have very small observational times, even zero, under some error scenarios. It means that this type of study is very important, since the observational data do not give very accurate values for the physical data of the bodies.

At the end, a search is made to find trajectories that have good observation times for all the error scenarios simulated, because they can be used as initial parking orbits for the spacecraft. Those orbits are defined as "Quasi-Stable Orbits". From those orbits, the spacecraft can make observations in any scenario, and a more accurate estimation of the sizes and masses of the asteroids is performed, allowing to make the final choices for the orbit of the spacecraft. Several orbits with this property were found. Good examples are Orbits 36, 45 and 56, but the best choice depends if the asteroid is at its periapsis or apoapsis. It was found that, for the initial orbit, it is better to use orbits with smaller observational times in the nominal situation, because they stay less time near the primaries, so they are less affected by the errors in the physical data. This fact makes them keep reasonable observational times in all the errors scenarios.

References

Aljbaae, S., et al.: The dynamical environment of asteroid 21 Lutetia according to different internal models. Mon. Not. R. Astron. Soc. **464**(3), 3552 (2017)

Araújo, R.A.N., Winter, O.C., Prado, A.F.B.A.: Sphere of influence and gravitational capture radius: a dynamical approach. Mon. Not. R. Astron. Soc. **391**(2), 675 (2008)

Araújo, R.A.N., et al.: Stability regions around the components of the triple system 2001SN263. Mon. Not. R. Astron. Soc. **423**(4), 3058 (2012)

Araújo, R.A.N., Winter, O.C., Prado, A.F.B.A.: Stable retrograde orbits around the triple system 2001 SN263. Mon. Not. R. Astron. Soc. **449**(4), 4404 (2015)

Bartczak, P., Breiter, S., Jusiel, P.: Ellipsoids, material points and material segments. Celest. Mech. Dyn. Astron. **96**(1), 31 (2006)

Bellerose, J., Scheeres, D.J., Restricted, J.: Full three-body problem: application to binary system 1999 KW4. J. Guid. Control Dyn. **31**(1), 162 (2008)

Belton, M.J.S., et al.: Galileo encounter with 951 Gaspra: first pictures of an asteroid. Science **257**(5077), 1647 (1992)

Belton, M.J.S., et al.: Galileo's encounter with 243 Ida: overview of the imaging experiment. Icarus **120**(0032), 1 (1996)

Broschart, S.B., Scheeres, D.J.: Control of hovering spacecraft near small bodies: application to asteroid 25143 Itokawa. J. Guid. Control Dyn. **28**(2), 343 (2005)

Broucke, R.A.: The celestial mechanics of gravity assist. In: AIAA/AAS Astrodynamics Conference, 88 (1988)

Broucke, R.A., Prado, A.F.B.A.: Jupiter swing-by trajectories passing near the Earth. Adv. Astronaut. Sci. **82**(2), 1159 (1993)

Brum, A.G.V., et al.: Preliminary development plan of the ALR, the laser rangefinder for the Aster deep space mission to the 2001 SN263 asteroid. J. Aerosp. Tehchnol. Manag. **3**(3), 331 (2011)

Byram, S.M., Scheeres, D.J.: Stability of Sun-synchronous orbits in the vicinity of a comet. J. Guid. Control Dyn. **32**(5), 1550 (2009)

Fieseler, P.D.: A method for solar sailing in a low Earth orbit. Acta Astronaut. **43**(9–10), 531 (1988)

Gomes, V.M., Prado, A.F.B.A.: Swing-by maneuvers for a cloud of particles with planets of the solar system. WSEAS Trans. Appl. Theor. Mech. **3**(11), 869 (2008)

Holman, M.J., Wiegert, P.A.: Long-term stability of planets in binary systems. Astron. J. **117**, 621 (1999)

Hu, W., Scheeres, D.J.: Numerical determination of stability regions for orbital motion in uniformly rotating second degree and order gravity fields. Planet. Space Sci. **52**, 685 (2004)

Huntress, W., et al.: The next steps in exploring deep space—a cosmic study by the IAA. Acta Astronaut. **58**, 304 (2006)

Johnston's Archive. (276049) 2002CE26. Available in http://www.johnstonsarchive.net/index.html. Access in 24 Oct. 2016

Jones, T., et al.: Asteroid system 2001 SN263. In: 42nd Lunar and Planetary Science (2011)

Kuga, H.K., Kondapalli, R.R., Carrara, V.: Introdução à Mecânica Orbital. 2. In: dos Campos, S.J. (ed.) INPE, p. 67 (2012) (sid.inpe.br/mtcm05/2012/06.28.14.21.24-PUD). Available in http://urlib.net/8JMKD3MGPAW/3C76K98. Access in 24 abr. 2016

Masago, B.Y.P.L.: Estudo de órbitas ressonantes no sistema triplo 2001SN$_{263}$. Dissertation of Master degree (in portuguese), INPE (2014)

Masago, B.Y.P.L., et al.: Developing the "Precessing inclined bi-elliptical four-body problem with radiation pressure" to search for orbits in the triple asteroid 2001SN263. Adv. Space Res. **57**, 962 (2016)

Mudryk, L.R., Wu, Y.: Resonance overlap is responsible for ejecting planets in binary systems. Astrophys. J. **639**, 423 (2006)

Murray, D.C., Dermott, S.F.: Solar System Dynamics p. 591. Cambridge University Press, New York (1999)

Prado, A.F.B.A.: A comparison of the "patched-conics approach" and the restricted problem for Swing-bys. Adv. Space Res. **40**, 113 (2007)

Prado, A.F.B.A.: Mapping swing-by trajectories in the triple asteroid 2001SN$_{263}$. In: 13th International Conference on Space Operations. American Institute of Aeronautics and Astronautics, Reston (2014a)

Prado, A.F.B.A.: Mapping orbits around the asteroid 2001SN$_{263}$. Adv. Space Res. **53**, 877 (2014b)

Prado, A.F.B.A., Broucke, R.A.: Transfer orbits in restricted problem. J. Guid. Control Dyn. **18**(3), 593 (1995)

Rossi, A., Marzari, F., Farinella, P.: Orbital evolution around irregular bodies. Earth Planets Space **51**(11), 1173 (1999)

Scheeres, D.J.: Dynamics about uniformly rotating triaxial ellipsoids: application to asteroids. Icarus **121**, 67 (1994)

Scheeres, D.J.: Orbital Motion in Strongly Perturbed Environments. Springer, Berlin (2012a). ISBN 978-3-642-03255-4

Scheeres, D.J.: Orbit mechanics about asteroids and comets. J. Guid. Control Dyn. **35**(3), 987 (2012b)

Scheeres, D.J.: Orbital mechanics about small bodies. Acta Astronaut. **72**, 1–14 (2012c)

Scheeres, D.J., Hu, W.: Secular motion in a 2nd degree and order gravity field with no rotation. Celest. Mech. Dyn. Astron. **79**(3), 183 (2001)

Shang, H., Wu, X., Cui, P.: Periodic orbits in the doubly synchronous binary asteroid systems and their applications in space missions. Astrophys. Space Sci. **355**, 69–87 (2015)

Sukhanov, A.A., et al.: The aster project: flight to a near-Earth asteroid. Cosm. Res. **48**(5), 443 (2010)

Surovik, D.A., Scheeres, D.J.: Autonomous maneuver planning at small bodies via mission objective reachability analysis. In: AIAA/AAS Astrodynamics Specialist Conference (2014)

Veverka, J., et al.: The landing of the Near-Shoemaker spacecraft on asteroid 433 Eros. Nature **413**(6854), 390 (2001)

Werner, R.A.: The gravitational potential of a homogeneous polyhedron or don't cut corners. Celest. Mech. Dyn. Astron. **59**(3), 253 (1994)

Yang, H., Gong, S., Baoyin, H.: Two-impulse transfer orbits connecting equilibrium points of irregular-shaped asteroids. Astrophys. Space Sci. **357**, 66 (2015)

Yoshikawa, M., Fujiwara, A., Kawaguchi, J.: Hayabusa and its adventure around the tiny asteroid Itokawa. Proc. Int. Astron. Union **2**, 323 (2007)

Zeng, X., Baoyin, H., Li, J.: Updated rotating mass dipole with oblateness of one primary (II): out-of-plane equilibria and their stability. Astrophys. Space Sci. **361**, 15 (2016)